IEEE Access
Multidisciplinary | Rapid Review | Open Access Journal

Received July 24, 2019, accepted July 30, 2019, date of publication August 12, 2019, date of current version August 23, 2019.

Digital Object Identifier 10.1109/ACCESS.2019.2934406

Study on Spatial-Temporal Distribution Characteristics of the Discharge Process in a 1 m Rod-Plate Gap Under Different Polarity Lightning Impulses

YAQI ZHANG[1], (Member, IEEE), YONGXIA HAN[1], (Member, IEEE), WENBO ZHENG[1], JIE YANG[1], LU QU[2], GANG LIU[2], XIANGEN ZHAO[2], AND LICHENG LI[1]

[1]School of Electric Power, South China University of Technology, Guangzhou 510640, China
[2]Electric Power Research Institute, China Southern Power Grid, Guangzhou 510080, China

Corresponding author: Yongxia Han (epyxhan@scut.edu.cn)

This work was supported in part by the National Natural Science Foundation of China under Grant 51541704, and in part by the National Engineering Laboratory for Ultra High Voltage Engineering Technology, Kunming, Guangzhou, under Grant NEL201704.

ABSTRACT The observation of the air gap discharge process is the basis of revealing the physical mechanism of gas discharge and establishing the accurate numerical simulation model. In order to obtain the variation characteristics at different development stages during the air gap discharge processes under positive and negative lightning impulses in this paper, repetitive discharge tests of 1 m rod-plate air gap under standard lightning impulse were carried out in the National Engineering Laboratory (Kunming) for Ultrahigh-voltage Engineering Technology. An improved discharge observation method, using electron-multiplying intensified charge-coupled device (EMICCD) camera, was adopted in the test. A series of discharge spatial-temporal distribution images with nanosecond exposure time and interval time were captured by changing the shooting time delay of the EMICCD in repetitive discharges. The complete discharge development process was reproduced by the image stitching. The development process and the characteristics of the air gap discharge under lightning impulse were analyzed qualitatively. The characteristics of the measured discharge current under the positive lightning impulse were discussed. The testing results and the analysis show that the shape and the development process of the ionization region of the streamer are quite different under different lightning impulses. There are spherical and fan-shaped streamer regions under the positive and negative lightning impulse, respectively. After the streamer runs through the entire gap, the leader develops from the rod electrode to the plate electrode (under the positive impulse) or from both the rod and the plate electrode to the middle area (under the negative impulse). Then the final jump occurs and the gap is broken down. If the streamer still cannot penetrate the entire gap when the applied impulse voltage exceeds the peak, the gap will not be broken down finally.

INDEX TERMS Spatial-temporal distribution with nanosecond exposure time, current measurement, EMICCD, standard lightning impulse, the microscopic process of discharge.

I. INTRODUCTION

Research on the discharge mechanism, the experimental observation and the numerical simulation of long air gap is the basis of external insulation design in the power system [1]–[7]. The macroscopic and microscopic observation of discharge development process is the foundation of discharge mechanism and numerical simulation.

The Les Renardieres research group had carried out a systematic and comprehensive experimental study on 1.5-10 m air gap discharges under the positive and negative switching impulse [8]–[11]. They established a relatively complete set of observation and measurement methods. A large number of parameters and physical characteristics in the long gap

The associate editor coordinating the review of this article and approving it for publication was Nagarajan Raghavan.

discharge process were obtained. Presented with the image results, the stages of initial corona, streamer, leader and final jump in the discharge process were proposed, and the initiation and development of each discharge stage under the switching impulse were described. Meanwhile, 'space leader' was used to explain the stepped leader development of the long gap discharge under negative impulse [12], [13]. However, limited by test conditions and equipment functions, the exposure time and the time interval (microsecond level) of most discharge observation systems is unsuitable for the instantaneous observation of the faster discharge process in a long gap. Researches reflecting the complete discharge development process, especially with weak discharge light, are insufficient [14], [15].

Nowadays, more advanced observation devices and measurement system have been applied to observe the discharge process and measure the discharge parameters in the long air gap [16]–[19]. Firstly, the charge-coupled device (CCD) camera is used. Its shooting time interval is more than 2 μs and the exposure time is about 1 μs. The CCD camera has been widely used to observe the macroscopic characteristics of the leader discharge process in the long gap under the impulse with long voltage duration [20]–[27]. Yingzhe Cui *et al*. observed the expansion process of the leader channel near the rod electrode in 1 m air gap under the positive lightning impulse, with the shooting range of gap length being 5.5−11.7 mm only [28]–[30]. In their study, the CCD was used along with Mach-Zehnder interferometer. However, for the whole gap observation of the discharge process under the lightning impulse with faster voltage rise and shorter breakdown time, the shooting and exposure time of the CCD are still not short enough to capture weak discharge. Therefore, the intensified charge-coupled device (ICCD) with higher spatial and temporal resolution has been utilized to study the transient discharge process of lightning impulse. The ICCD camera has the continuous shooting time and exposure time at nanosecond level and can capture the weak corona and streamer development by increasing light intensity gain. However, the ICCD still has some deficiencies. When the time interval of continuous shooting is short, the shooting range will be greatly reduced. Medeiros P T and She Chen *et al*. respectively observed the streamer breakdown process in 2-6 cm nitrogen gap and the unbreakdown streamer discharge process of a 57 cm rod-plate air gap under lightning impulse [31]–[33]. Ali Shirvani *et al*. adopted a new high-speed camera system and observed the streamer and leader development of 2-4 m rod-plate air gap discharges under the 1.2/50 μs positive lightning impulse. The discharge process included four stages: first streamer, second streamer, reverse streamer and leader. The shortest shooting time interval and the exposure time were both 20 ns and the shooting range of gap length was only 25 cm during streamer development process. Nevertheless, the shooting time interval was up to 1 μs when the shooting range included the whole gap during the leader development process [34], [35]. The above analysis shows that the spatial-temporal distribution image observation with nanosecond exposure time and time interval under the lightning impulse has been realized using multiple ICCD cameras. However, in the continuous shooting mode with one ICCD camera, there is still a contradiction between the shooting range of the discharge and the shooting time interval, which may cause some difficulties in the detailed observation of the instantaneous change of charge in the long gap discharge process. The shooting image range is limited in some experiments, and the light intensity gain of ICCD cannot be adjusted with the discharge development. Through individual image recorded in each discharge, P O Kochkin *et al*. captured the discharge process of 1 m air gap between two conical electrodes. They obtained different discharge images with the exposure time of 60-1000 ns [36], [37]. Until now, there are few experiments using ICCD to record individual images with 1 m rod-plate air gap under the lightning impulse.

The purpose of this paper is to obtain detailed variation characteristics at different stages during the long air gap discharge processes under the positive and negative lightning impulses. An improved discharge observation method was designed to carry out the repetitive discharge test of 1 m rod-plate air gap under standard lightning impulse at the indoor test site of the National Engineering Laboratory of UHV Engineering Technology (Kunming). The electron-multiplying intensified charge-coupled device (EMICCD) camera, with the exposure time at nanosecond level, was used to capture the discharge image with nanosecond spatial-temporal distribution. Clear discharge images were obtained through changing the EMICCD time delay and the light intensity gain; and the complete discharge processes are reproduced by the image stitching. In order to ensure the repeatability of the test results and reduce the impact of discharge dispersion, a large number of observed data and images during discharge process at different impulse voltage levels and polarities are obtained and analyzed. The characteristics of the measured discharge current under the positive lightning impulse are discussed. The characteristics and the laws of the 1 m rod-plate air gap discharge under positive and negative standard lightning impulses are proposed based on the results of statistical analysis, which improves and complements the understanding of the microscopic process of the long gap discharge.

II. TEST METHOD

A. TESTING DEVICE AND MEASURING SYSTEM

The test of 1 m rod-plate air gap under lightning impulse was carried out at the indoor test site of the National Engineering Laboratory of UHV Engineering Technology (Kunming) with an altitude of 2100 m [38]. The test device mainly included an impulse voltage generator, a voltage divider, an oscilloscope, an EMICCD, and a 1m rod-plate gap. The testing circuit is shown in Figure 1.

The standard lightning impulse of 1.2/50 μs was produced by the 1600 kV impulse voltage generator with the rated capacity of 320 kJ. The impulse voltage generator has

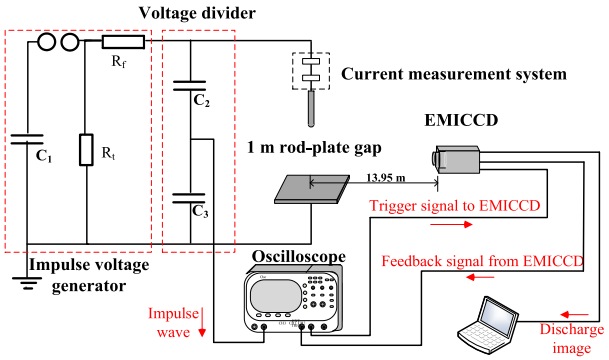

FIGURE 1. The testing circuit.

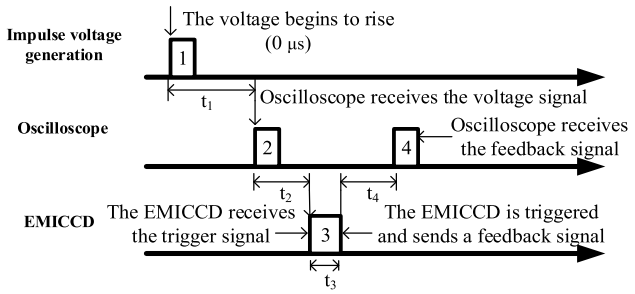

FIGURE 2. The timing diagram of the synchronous trigger system.

eight charging stages and the main capacitor and the charging voltage of each stage are 2 μF/ 200 kV. The wave head resistance is 40 kΩ, and tail resistance is 3.8 kΩ. The EMICCD model is Princeton Instruments PI-MAX4 with a precise control to exposure time and trigger delay. Its minimum shutter trigger delay and exposure time are 26 ns and 2.88 ns. The EMICCD can also simultaneously output shutter switch signal (Feedback signal from the EMICCD). This detector has a high signal-to-noise ratio and a good linearity of light intensity gain. The EMICCD is equipped with Nikon standard zoom lens with a focal length of 24-70 mm and a maximum aperture of F2.8. The head of the rod electrode is spherical with a diameter of 3.75 cm. And the length of the rod is about 30 cm. The plate electrode is 3×3 m iron plate. The whole gap is located in the darkroom to ensure the safety of the test and the accuracy of the shooting. A time-resolved digital optical measurement system was used to record the discharge current. This measurement system includes a coaxial current sensor and a digital fiber transmission system [39]–[41].

Based on the above test equipment, the test was conducted in accordance with the IEC test and measurement methods [42], [43].

In order to synchronize the electric signal with the optical signal, the oscilloscope was used for triggering the EMICCD synchronously. The timing diagram of the synchronous trigger system is illustrated in Figure 2. The transmission time from the beginning of the impulse voltage generated by the impulse generator to the receiving of the voltage signal by the oscilloscope is t_1. The transmission time that the oscilloscope sends a trigger signal to the EMICCD is t_2. The trigger delay set in the EMICCD is t_3. The transmission time that the EMICCD feedback signal sends to the oscilloscope is t_4.

TABLE 1. The testing conditions.

Discharge research objects	Preset impulse voltage level (kV)	Shooting interval (ns)	Exposure time (ns)
$U_{50\%}$	--	--	--
Complete breakdown discharge processes	+616 +784 +1232 -840 -1040	100	10
The discharge stages of initial corona and streamer	+616 -840	50	
The discharge stages of leader and final jump	+616 -1040	100-200	
Unbreakdown discharge processes	+400 -640	100	

B. TESTING CONTENT

The complete process of 1m rod-plate air gap discharge under standard lightning impulses at different voltage levels was photographed by the above measurement system.

The 50% impulse discharge voltage ($U_{50\%}$) of 1m rod-plate gap discharge were conducted first to set reasonable impulse voltage levels in the following test. According to the $U_{50\%}$ test results, there are several voltage levels higher than $U_{50\%}$ and two voltage levels lower than $U_{50\%}$ were chosen for the image shooting of the discharge processes under positive and negative lightning impulses. The testing conditions of are shown in Table 1.

Considering the limitation of the continuous shooting mode of the EMICCD, only one image was taken at a time. By setting different EMICCD trigger delay and light intensity gain in shooting during repeated discharge processes at the same voltage level, the discharge development of the rod-plate gap with time were observed. The EMICCD exposure time was set to 10 ns in the test on the basis of the exposure time stability test results. The light intensity gain of the EMICCD was adjusted for each shoot to observe the streamer and leader processes with large difference in light intensity. The shooting range included the whole gap. Therefore, the difference of the instantaneous ionization region morphology and the change process of the ionization degree in discharge was captured in detail. And the whole discharge processes were reproduced by images stitching. There were about 1903 effective images obtained in total in order to avoid the influences of the discharge dispersion and the randomness on the test results.

Due to tolerance capacity limitation of the sustained heavy current of the current measurement system, only part of the discharge current under the positive lightning impulse at + 616 kV voltage level were recorded. These data were discussed as a complementary explanation in Part IV.

During the test, the indoor temperature was between 22°C and 26°C, the relative humidity was between 56% and 74%, and the air pressure was between 78.98kPa and 79.01kPa.

III. TEST RESULTS

The spatial-temporal distribution characteristics and ionization degree of different discharge stages are analyzed by the discharge images obtained. The analysis is divided into three parts. The first part illustrates the $U_{50\%}$ and the volt-second characteristics of the 1 m rod-plate air gap under the lightning impulses. The second part focuses on initial corona and streamer discharges with weak light intensity, and the third part focuses on leader and final jump discharges with intense light intensity.

The discharge images are in form of contour maps. The different color lines in the images represent different light intensity ranges. The shooting time (T), time delay (Td), maximum light intensity (I) of the discharge channel, and morphological parameters of the ionization area are indicated in each image. The starting point of the voltage rise is taken as the time reference (0 μs). It is calculated by the relative time difference between voltage waveform and the EMICCD trigger signal. The light intensity shown in the images have been converted to the same value as in the case of no gain.

A. $U_{50\%}$ AND THE VOLT-SECOND CHARACTERISTICS

The $U_{50\%}$ under the positive and negative impulses are 533.76 kV and 788.12 kV, respectively.

In order to compare the characteristic differences of discharge in altitude. The volt-second characteristics of the 1 m rod-plate air gap under the positive and the negative lightning impulses are illustrated in Figure 3.

All the data was corrected in temperature and humidity. The data in volt-second characteristics with altitude correction was corrected in temperature, humidity, and altitude [44], [45].

As shown in Figure 3, the volt-second characteristics under the two polarity impulses are quite different. And the breakdown voltages in high altitude area are lower than those on the plains. The relative analysis of the discharge characteristics and flashover criterion in high altitude were in Reference [45]–[47].

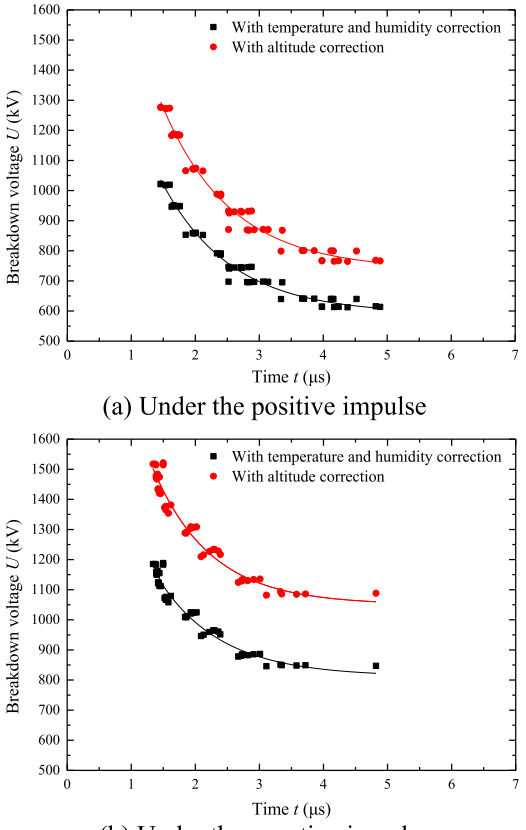

FIGURE 3. The volt-second characteristics of 1 m rod-plate air gap under the standard lightning impulses.

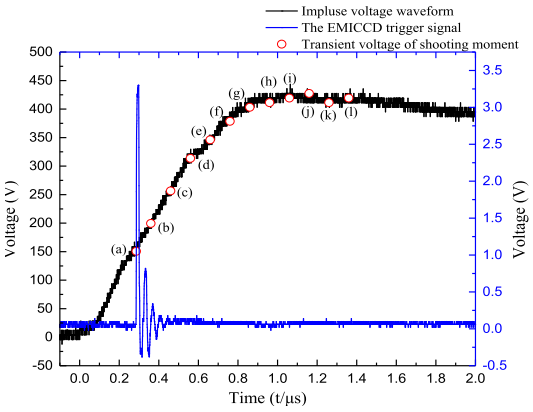

FIGURE 4. Relative position of the + 400 kV voltage level impulse voltage waveform and the EMICCD trigger signal.

B. INITIAL CORONA AND STREAMER DISCHARGES

Taking the unbreakdown discharge and the initial corona and the streamer stages during the breakdown discharge processes under the positive and negative lightning impulses as examples, the differences of morphological characteristics and ionization degree between the breakdown and the unbreakdown discharge processes are analyzed comparatively. And the development laws of the initial corona and the streamer stages during 1 m rod-plate air gap discharge process are revealed.

1) POSITIVE DISCHARGE

The testing lightning impulse waveforms of + 400 kV and + 616 kV voltage levels are shown in Figure 4 and Figure 6 respectively. The corresponding actual trigger signals with the EMICCD delay set to 26 ns are indicated in these two figures. Figure 5 and Figure 7, including

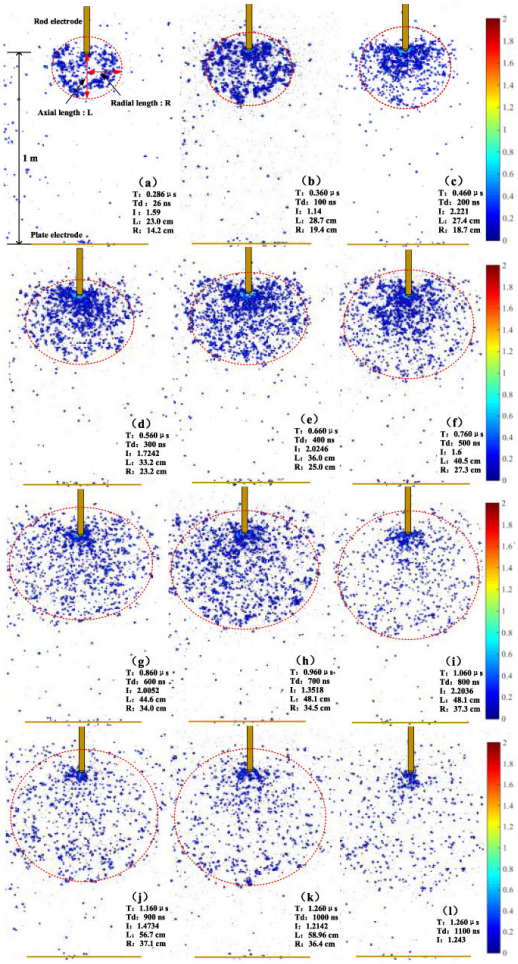

FIGURE 5. The unbreakdown discharge process at + 400 kV voltage level.

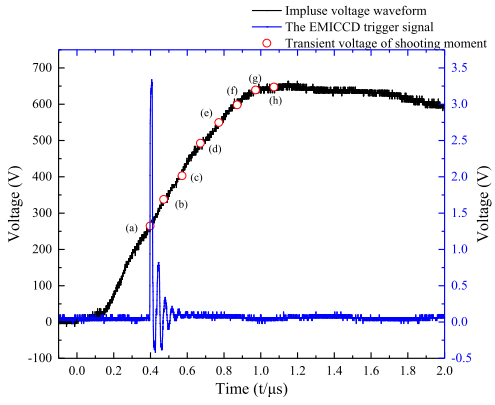

FIGURE 6. Relative position of the + 616 kV voltage level impulse voltage waveform and the EMICCD trigger signal.

a series of discharge images at different shooting times, are the unbreakdown discharge process at + 400 kV voltage level and the initial corona and the streamer stages of the breakdown discharge process at + 616 kV voltage level. Meanwhile, the theoretical instantaneous impulse voltage positions corresponding to image shooting times are marked in Figure 5 and Figure 7. The relative humility was

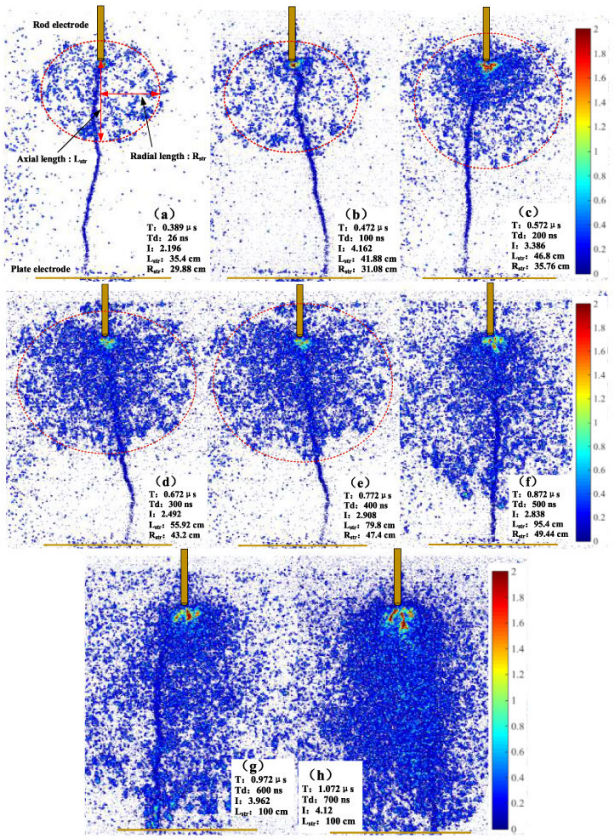

FIGURE 7. The initial corona and the streamer stages during the breakdown discharge process at + 616 kV voltage level.

between 66% and 70% during the test at + 400 kV voltage level and between 56% and 61% during the test at + 616 kV voltage level.

Figure 5 and Figure 7 show that the unbreakdown discharge processes is similar to the initial corona and the streamer stages of the breakdown discharge process under positive lightning impulse. In both discharge processes, the spherical ionization regions near the head of the rod electrode (anode) are produced, and the ionization region gradually expands around with the increase of the impulse voltage. However, the density of charged particles and the light intensity in the ionization region during the unbreakdown process are significantly smaller than those in the ionization region during the breakdown process. When the impulse voltage decreases after reaching the peak during the unbreakdown process, the superimposed electric field formed by the impulse voltage and the existing space charge is insufficient to keep the continuous ionization. As a result, the ionization degree in the gap gradually weakens, and the existing electrons also disappear. The ionization region cannot develop to the plate electrode.

There is a weak penetrative channel in each image of the breakdown discharge process; however, it does not occur during the unbreakdown discharge process. After many tests, it was found that this penetrating channel was not a real discharge phenomenon captured at the shooting moment. It is the residual image left in the camera caused by the final

discharge breakdown channel. It appeared because the intense luminescence of the main discharge channel occurs at the breakdown moment. Even if the electronic shutter of the EMICCD camera had been closed, part of the light could still reach the photographic plate in the camera. The similar phenomenon also appears in the discharge images taken by ICCD in [36], [37].

The first image is captured at 0.389 μs (Figure 7(a)) during the breakdown discharge process. An intense spherical ionization region begins to appear near the head of the rod electrode. With the rising of the impulse voltage applied on the rod electrode, the streamer area gradually expands around from the head of the electrode rod. At about 0.972 μs (Figure 7(g)), the streamer reaches the plate electrode (cathode). During the development of the streamer, the axial length of the streamer increases gradually. The estimated average velocity of the streamer is 0.17 cm/ns. At 0.398-0.772 μs (Figure 7(a)-(e)), the radial length of the streamer is expanding outwards, and the expansion rate is 0.05-0.10 cm/ns. However, the radial length increases slightly after 0.772 μs. When the streamer reaches the plate electrode, the main ionized area in the streamer is concentrated in the axial direction and the radial length decreases slightly.

In the streamer region, the farther away from the head of the rod electrode, the weaker the ionization degree. The maximum intensity at the head of the rod electrode increases with oscillatory behavior. After 0.972 μs, besides the overall charge density and light intensity, the range of the intense ionization region around the rod head also begins to expand obviously. A few of the intense ionization regions will also appear near the plate electrode. The light intensity of the streamer in Figure 7 is below 5. From 1.072 μs (Figure 7(h)), the intense ionization region begins to change from spherical to long strip shape and extend downwards, indicating that the leader has formed at this time.

In References [36], [37], [48], the individual image shooting method was adopted. The streamer and leader discharge process of the electrode head were studied. In the streamer observation of a 4-cm gap, the development process of positive polarity streamer discharge was obtained. However, the image size range is limited. In addition, the ionized regions in some images with long exposure time are filamentous. This phenomenon should be due to the accumulation of light intensity over a long period of time. Therefore, it can also be inferred that the exposure time will directly affect the morphology of ionized regions in the observed discharge images.

2) NEGATIVE DISCHARGE

The testing lightning impulse waveforms of − 640 kV and −840 kV voltage levels are shown in Figure 8 and Figure 10 respectively. The corresponding actual trigger signals with the EMICCD delay set to 26 ns are indicated in these two figures. Figure 9 and Figure 11 are the unbreakdown discharge process at the − 640 kV voltage level and the initial corona and the streamer stages of the breakdown discharge process

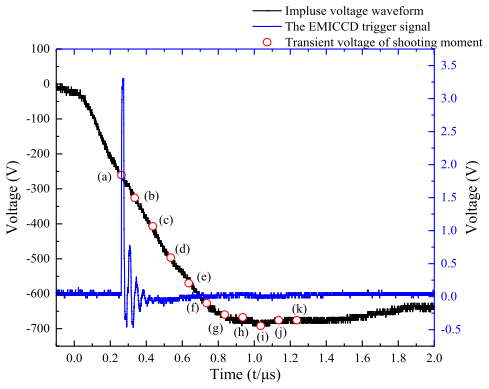

FIGURE 8. Relative position of the − 640 kV voltage level impulse voltage waveform and the EMICCD trigger signal.

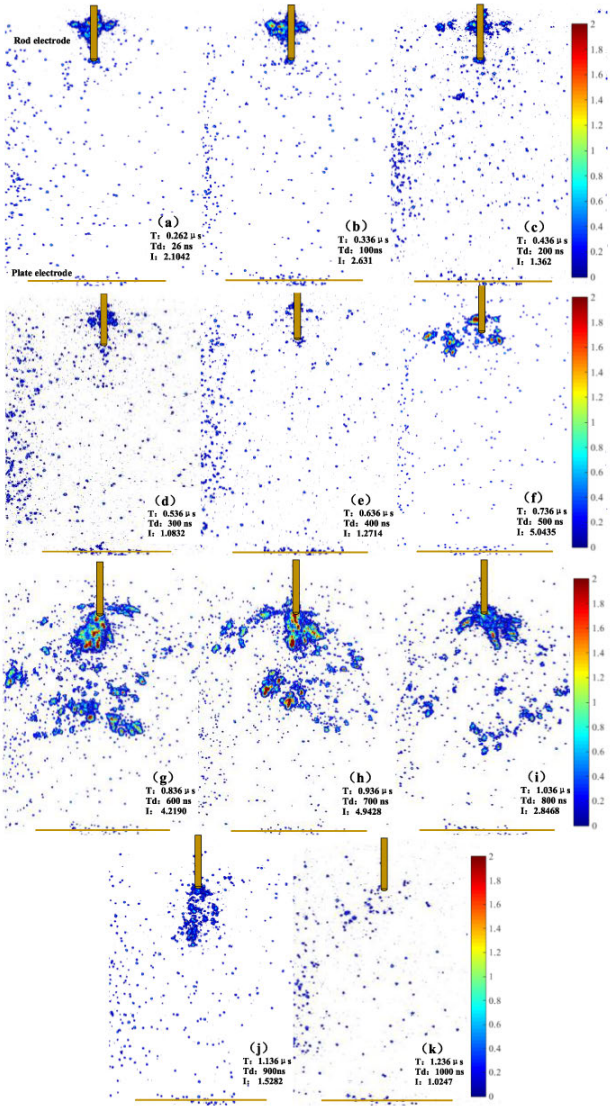

FIGURE 9. The unbreakdown discharge process at − 640 kV voltage level.

at the − 840 kV voltage level. Figure 9 and Figure 11 include a series of discharge images at different shooting times. Meanwhile, the theoretical instantaneous impulse voltage

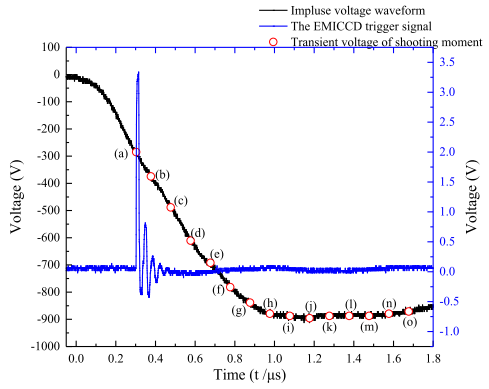

FIGURE 10. Relative position of the −840 kV voltage level impulse voltage waveform and the EMICCD trigger signal.

positions corresponding to image shooting times are marked in Figure 8 and Figure 10. The relative humility during the tests were about 68% at − 640 kV voltage level and about 64% at − 840 kV voltage level.

Figure 9 and Figure 11 show that the process of unbreakdown discharge is similar to the initial corona and the streamer stages during the breakdown discharge process under the negative lightning impulse. The weaker ionization region occurs around the head of the rod electrode (cathode) at first. While the relatively intense and obvious ionization region occurs above the head of the rod subsequently; there is no intense ionization between the rod and the plate. This phenomenon may be caused by a superimposed electric field due to space charges and original electric field. With the increase of voltage, a fan-shaped ionization region forms near the rod electrode and develops towards the plate electrode (anode). However, the density of charged particles and light intensity in the ionization region during the unbreakdown process are significantly smaller than those during the breakdown process. If the superimposed electric field formed is insufficient to keep the continuous ionization, the ionization in the gap will gradually weaken and the existing electrons will also disappear.

During the breakdown discharge process under the negative lightning impulse in Figure 11, the beginning of the initial corona is relatively slow, which is recorded in Figure 11(a)-(c). At 0.577-0.677 μs (Figure 11(d)-(e)), an ionization area with a discus shape occurs above the head of the rod electrode. At 0.777-1.577 μs (Figure 11(f)-(n)), intense ionization begins to appear near the head of the rod and extends downwards. This is the negative streamer. Unlike the positive streamer, the ionization region of the negative streamer is fan-shaped. It mainly extends to the plate electrode along the axis. Due to the large dispersion of the negative discharge, the continuity of the images shot is worse than that of the positive discharge. And the axial length development of the streamer is unstable in Figure 11. The estimated average velocity of the negative streamer is 0.22 cm/ns.

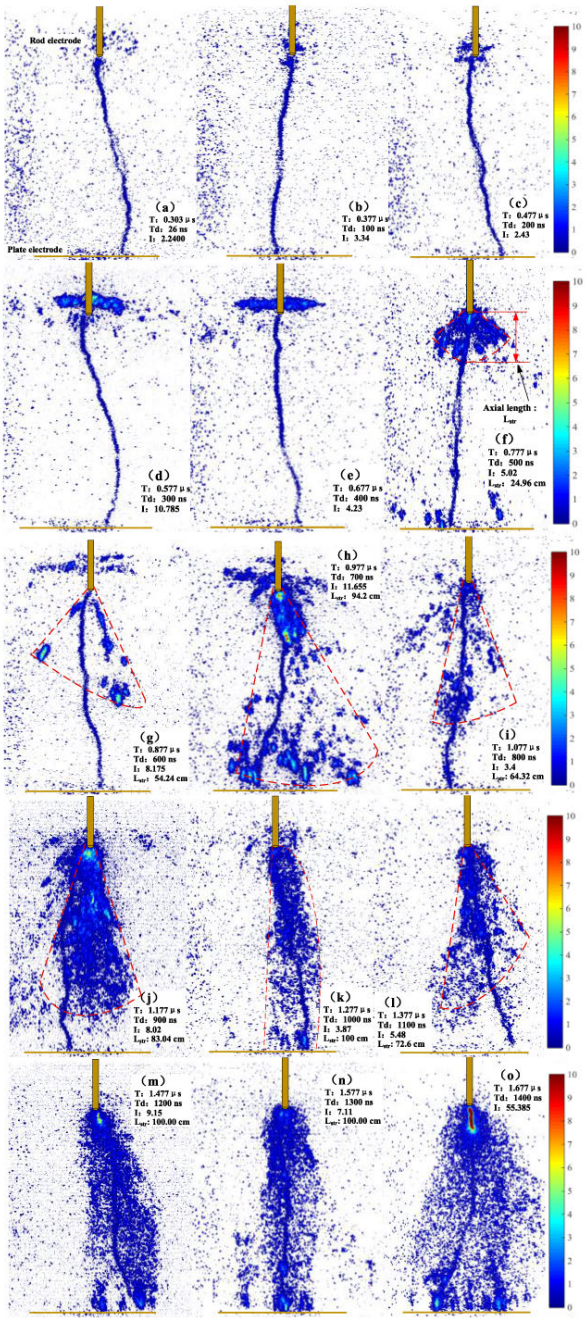

FIGURE 11. The initial corona and the streamer stages during the breakdown discharge process at − 840 kV voltage level.

A large number of free electrons is generated during the negative streamer development, which moves from the circumference to the plate electrode. Therefore, the concentrated intense ionization region not only appears around the head of the rod electrode where a larger electric field exists, but also a large droplet-like intense ionization region forms at the streamer head. At 1.477-1.577 μs (Figure 11(m)-(n)), a penetrating streamer channel forms. The light intensity at both ends of the rod-plate gap becomes larger, which means the intense ionization region exists at both ends of the gap. Because of the uniform electric field of the plate electrode,

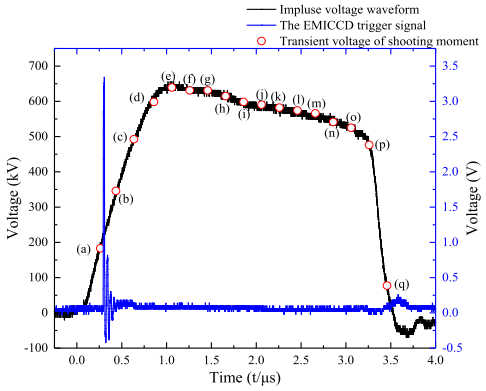

FIGURE 12. Relative position of the + 616 kV voltage level impulse voltage waveform and the EMICCD trigger signal.

a few intense ionization regions can be generated at the same time near the plate pole, and their positions and quantities generated are random. An upward leader probably forms from one of the intense ionization regions. The light intensity of the streamer in Figure 11 is below 10. With the continuous application of the impulse voltage, the ionization degree of the streamer channel increases further. Figure 11(o) and the change of light intensity shows that the discharge is more intense during this period, and the leader begins to form.

C. LEADER AND FINAL JUMP DISCHARGE

Taking the leader and the final jump stages during the breakdown discharge processes under the + 616kV and − 1040 kV lightning impulses as examples, the development processes after the streamer stage in the rod-plate gap discharge are studied. A fine nail is added above the plate as an arc-ignition device to ensure the stability of the leader development path. The actual length of the gap is shortened to 93 cm.

1) POSITIVE DISCHARGE

The testing lightning impulse waveform of + 616 kV voltage level is shown in Figure 12, and the corresponding actual trigger signal of the EMICCD delay set to 26 ns is indicated in this figure. Figure 13, including a series of discharge images at different shooting times, are the leader and the final jump stages during the breakdown discharge process at + 616 kV voltage level. Meanwhile, the theoretical instantaneous impulse voltage positions corresponding to the image shooting times are marked in Figure 12. The relative humility was between 56% and 74%.

The relationship between the maximum light intensity of the discharge channel and the corresponding instantaneous impulse voltage is shown in Figure 14.

As shown in Figure 13 and Figure 14, the leader starts at about 0.859-1.059 μs (Figure 13(e)). At 1.059 μs, the impulse voltage reaches the peak value and the maximum light intensity increases by 165% compared with that

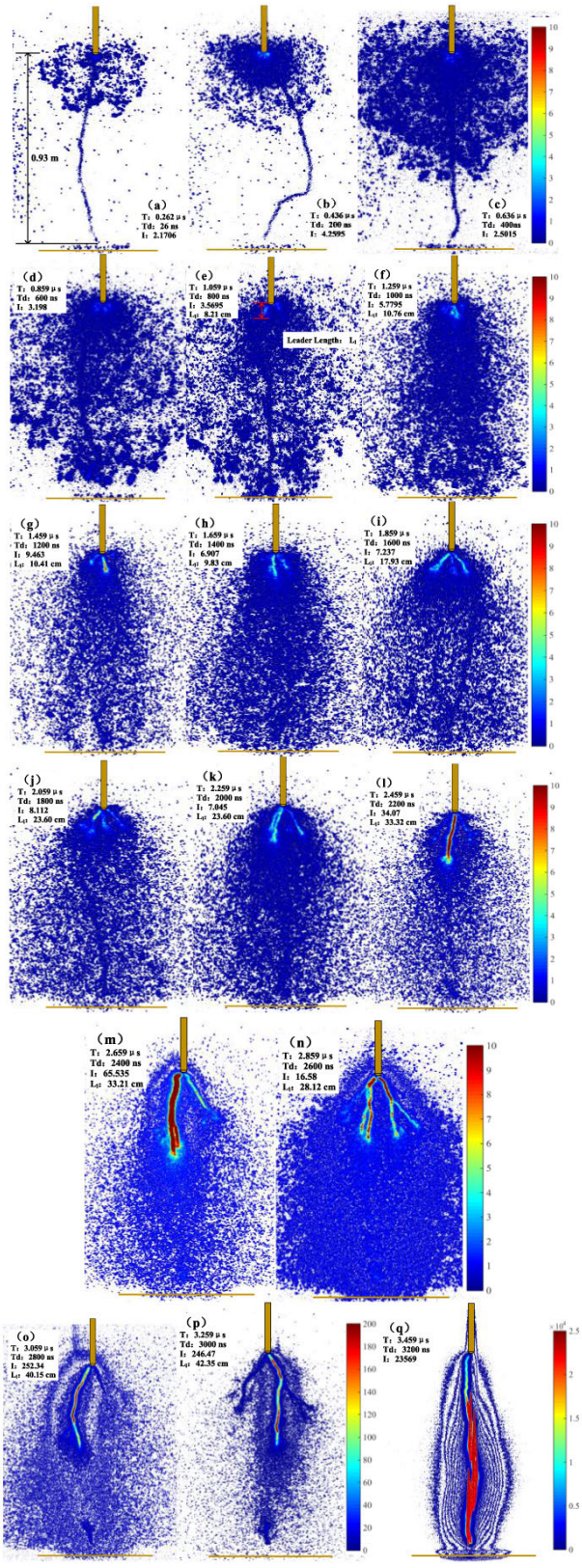

FIGURE 13. The leader and the final jump stages during the breakdown discharge process at + 616 kV voltage level.

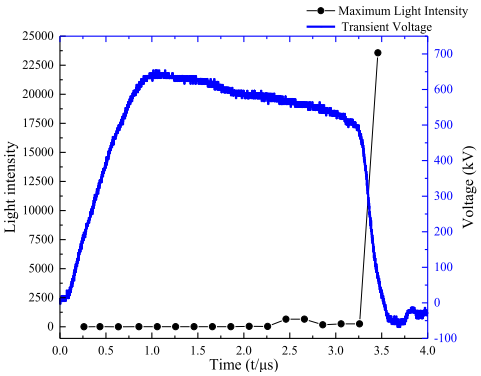

FIGURE 14. The relationship between the maximum light intensity of the discharge channel and the corresponding instantaneous impulse voltage.

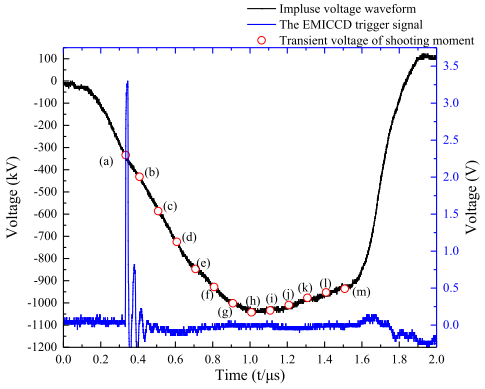

FIGURE 15. Relative position of the − 1040 kV voltage level impulse voltage waveform and the EMICCD trigger signal.

at 0.859 μs. And the intense ionization region originally gathered near the head of the rod electrode begins to extend downwards. A clear leader channel forms, which is called downward leader. The velocity of the downward leader is 0.018 cm/ns. With the gradual decrease of the impulse voltage, the leader continues to develop towards the plate. The development velocity decreases slightly while the maximum light intensity does not change much. The leader branches may occur in the process, and as for in Figure 13, 2-4 leader branches were captured. At 1.859-2.059 μs (Figure 13(i)-(j)), the maximum light intensity has a great jump again. At 2.059 μs, the maximum light intensity increases by 384% compared with that at 1.859 μs and the axial length of the leader increases to 23.6 cm. After 2.059 μs, the discharge of the main leader channel becomes more and more intense, while the other branches are obviously weakened. At 2.659μs (Figure 13(l)), due to the placement of the arc-ignition device, a week ionization region appears. At 2.859-3.459 μs (Figure 13(m)-(p)), when the downward leader develops, the ionization channel may gradually develop into an upward leader. However the light intensity (ionization degree) of upward leader is much weaker than that of the downward leader. The final jump discharge stage occurs during 3.259-3.459 μs, and the leader velocity reaches 0.248 cm/ns. At about 3.459 μs, the leader penetrates and the gap is broken down. The maximum light intensity increases to 23569.

2) NEGATIVE DISCHARGE

The testing lightning impulse waveform of − 1040 kV voltage levels is shown in Figure 15. And the corresponding actual trigger signal of the EMICCD delay set to 26 ns is indicated in this figure. Figure 16, including a series of discharge images at different shooting times, is the leader and the final jump stages during the breakdown discharge process at − 1040 kV voltage level. Meanwhile, the theoretical instantaneous impulse voltage positions corresponding to the image shooting times are marked in Figure 15. The relative humility was between 60% and 70%.

The relationship between the maximum light intensity of the discharge channel and the corresponding instantaneous impulse voltage is shown in Figure 17.

As shown in Figure 16 and Figure 17, the leader starts at about 0.908μs (Figure 16(g)), when the impulse voltage reaches the peak value and the maximum light intensity increases by 452% compared with that at 0.808 μs. As the impulse voltage decreases between 0.908μs and 1.408μs (Figure 16(h)-(l)), the downward leader continues to develop towards the positive plate electrode. The axial velocity and the maximum light intensity of the leader channel increase with oscillatory behavior. The downward leader velocity is less than 0.141 cm/ns and the maximum light intensity is less than 5130.The axial length of the leader varies considerably with the different shooting time. The individual frame shooting method can not reflect the negative discharge process with the large discharge dispersion very well. Comparing with the downward leader, the upward leader develops slowly. The final jump discharge stage occurs during 1.408-1.508 μs (Figure 16(l)-(m)), and the leader velocity reaches 0.422 cm/ns. At about 1.508 μs, the leader penetrates and the gap is broken down, and the maximum light intensity increases to 23778.

Comparing with the leader characteristics under the positive and negative lightning impulses, it can be found that the leaders under the lightning impulses with two polarities start to appear when the impulse voltages reach peak values, approximately when the breakdowns happened in wavetail. The similar phenomenon can be seen in Reference [48]. Two times of the distinct increase in the maximum light intensity are observed during the leader development. For the first time, the maximum light intensity of the positive leader increases by 165% and the negative leader increases by 452% when the leaders start to develop. For the second time, the maximum light intensity of the leaders increases to over 23000 when the leaders run through the gap.

IV. DISCUSSION

Based on the characteristics of discharge current, the inference of discharge process in the paper is further analyzed and verified. At the same time, there are some comparisons with other similar experiments. The differences and their causing reasons among them are analyzed. Through the analysis of

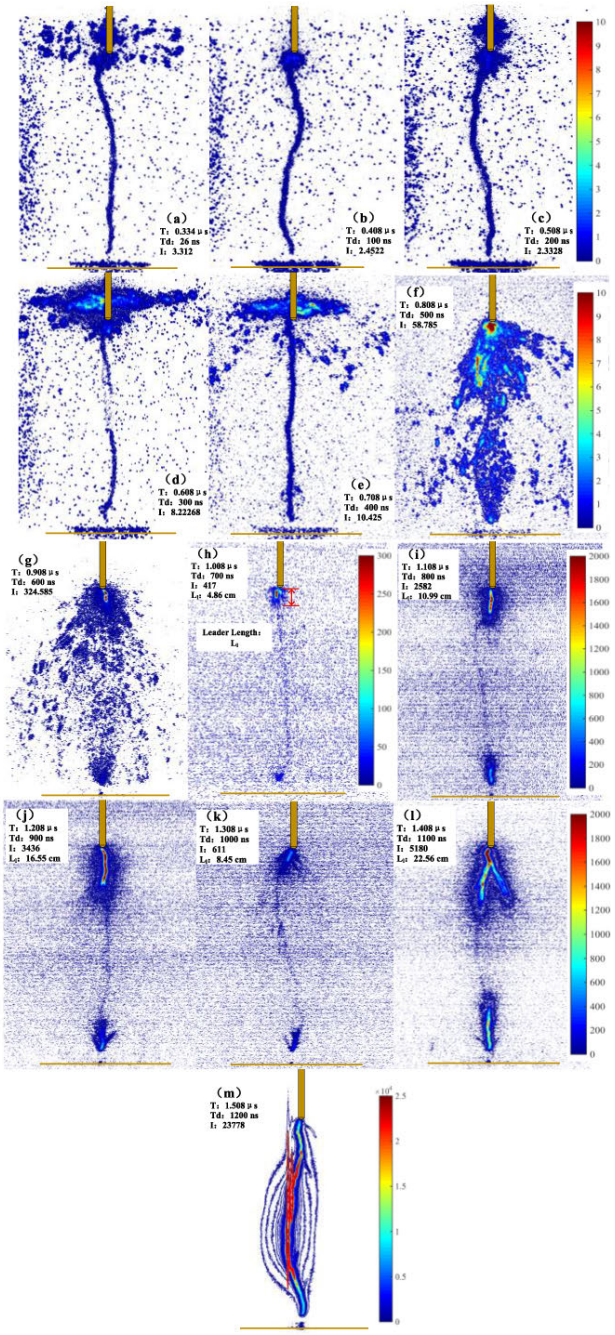

FIGURE 16. The leader and the final jump stages during the breakdown discharge process at − 1040 kV voltage level.

the testing results of the 1m rod-plate gap discharge under the lightning impulse, the detailed description and the difference analysis of the complete discharge processes under the positive and the negative impulses are as follows.

A. THE DISCHARGE CURRENT

Take the discharge process at +616 kV voltage level as an example, the impulse voltage, transient voltage of shooting moment, total current, and the displacement current are in shown the Figure 18.

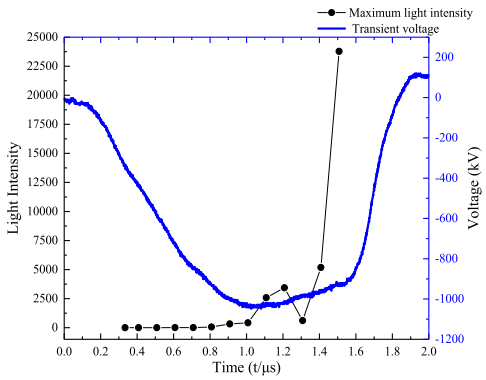

FIGURE 17. The relationship between the maximum light intensity of the discharge channel and the corresponding instantaneous impulse voltage.

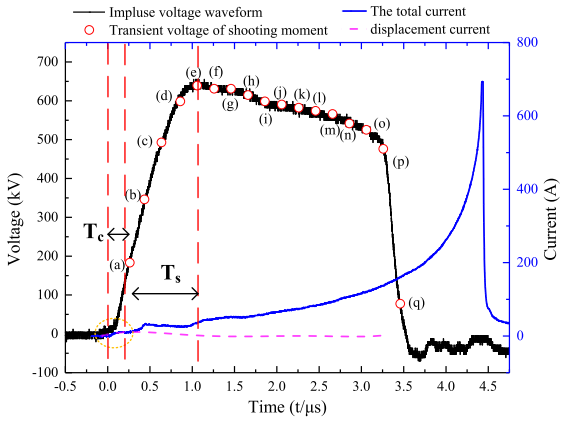

FIGURE 18. Discharge current and corresponding applied voltage of the + 616 kV breakdown process.

The impulse voltage and transient voltage of shooting moment are the same with those in Figure 12. The measured current is the total current i, which includes two parts. The following is the calculation function:

$$i = i_e + i_{dis} \tag{1}$$

where the streamer current i_e is related to charged particle motion, the displacement current i_{dis} is related to electrodes sets and the applied voltage [49].

The displacement current i_{dis} can be presented as follows:

$$i_{\text{dis}} = \text{C}_\text{g} \cdot \frac{\partial u}{\partial t} \tag{2}$$

where u is the applied voltage; C_g is the stray capacitance of the insulator string or air gap. When the applied voltage is low, the field strength at the head of the rod electrode is not strong enough to trigger intense ionization. At this time, all measured current is displacement current. After calculating, C_g in this test is estimated at about 12 pF.

As shown in Figure 18, during the early discharge process (T_c), the total current is equalled to the displacement current. It is the period of initial corona. The obvious streamer from the head of the rod electrode does not occur.

In the T_c time period, with the voltage rises continuously, the displacement current starts to decrease and close to zero. At the same time, the total current has a small rise. The reason is that the enhanced ionization and the ionization region expansion cause the increasing of the charged particles and the fast moving of electrons. The faster and continuous rise of the total current occurs after T_s when the applied voltage arrives near the peak value. It happens to be the beginning of the leader development process, which is described in the image analysis above. The total current rise exponentially when the gap is almost breakdown.

Different development stages of discharge process can be distinguished by the current analysis, and the analysis results are the same as the results of image analysis in Part III. In the streamer discharge stage, there is only a relatively gentle small rise, and then the current continues to rise because the leader discharge starts. This recorded current is different from the apparent streamer pulse current of the long gap discharge experiments mentioned in the literature [34], [35], [39], [40], [50]. Inferred from comparison, the difference is caused by the experimental conditions. According to the results of voltage, current and image analysis, the gap length of this discharge breakdown test is 1 m, and the electric field is relatively stronger, which leads to the rapid continuous development of the streamer to the plate electrode. When the streamer is about to penetrate the gap, ionization and energy accumulation near the head of the rod have reached the lead formation conditions. After the streamer penetration, the leader rapidly begins to develop downward and the current increases exponentially. Therefore, multiple streamer pulse currents do not exist during the rapid and continuous process of the streamer development and leader transformation. And there is no corresponding reverse ion wave (or second streamer) in the images captured indeed. Comparing the differences of current measurement experiments with that in this paper, the experimental conditions in the literatures that observed the streaming pulse current were either a gap with the length of more than 2 m [34], [35], [39], [40], a low voltage with a long duration [50], or an unbreakdown discharge process [34], [35], [50]. Detailed physical explanation of the differences needs to be further studied.

B. THE POSITIVE DISCHARGE

According to the nanosecond spatial-temporal distribution of the discharge process under the positive lightning impulse in 1 m rod-plate air gap, the complete discharge process is proposed, as shown in Figure 19.

Under the positive standard lightning impulse, when the initial electron collapse occurs near the head of the rod electrode with the increase of the applied voltage, the initial corona appears (Figure 19(a)). Subsequently, the number of the electron collapse and the spatial ionization degree gradually increases. The streamer begins to develop downward from the head of the rod electrode (Figure 19(b)) as the impulse voltage continues to increase. The strongest electric field around the head of the rod electrode leads to the maximum ionization. The free electrons move from the periphery to the head of the rod electrode, so the ionization region of the streamer appears to be spherical. The ionization degree around the central axis of the rod-plate gap is larger,

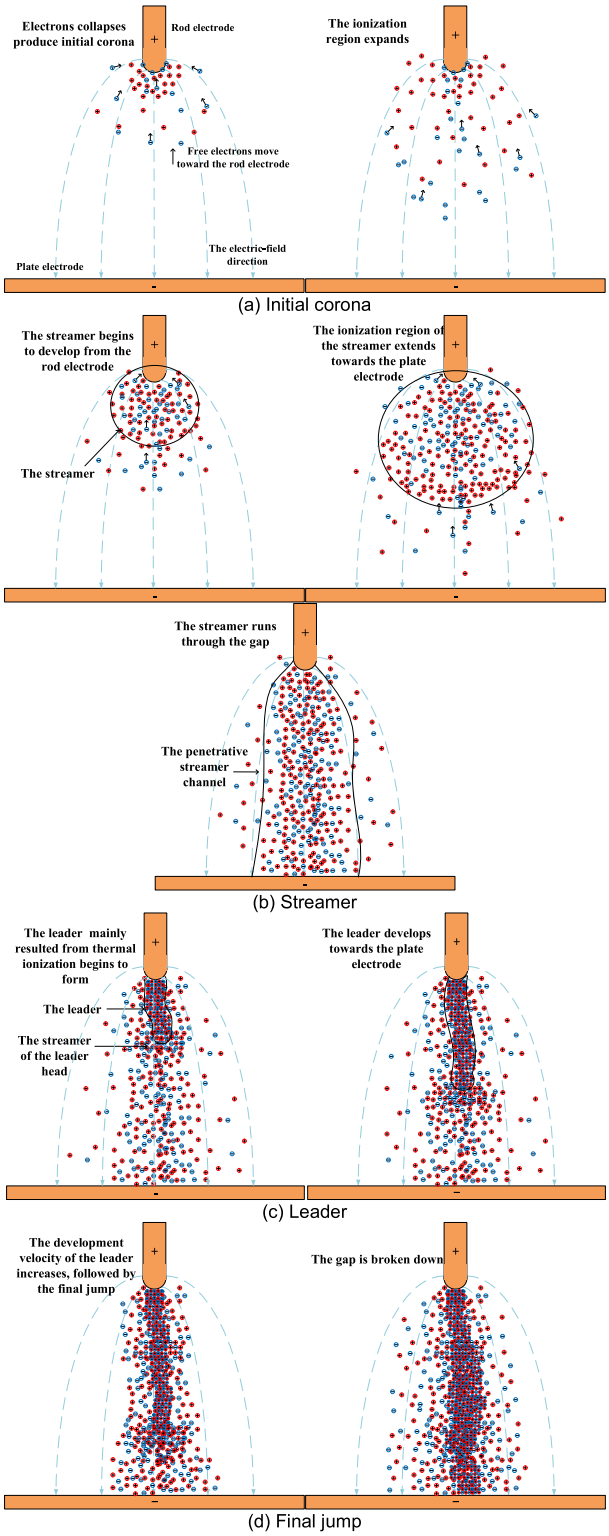

FIGURE 19. The breakdown discharge process of 1 m rod-plate gap under the positive lightning impulse.

but decreases with the increase of the distance from the central axis due to the electric field along the left and right sides of the axis is smaller. As the impulse voltage continues to rise, the ionization region of the streamer gradually enlarges and the ionization degree increases. The gap structure leads to a larger axial electric field in the gap, so the axial velocity of the streamer is much faster than the radial velocity. When the streamer extends and reaches the plate electrode, a penetrative streamer channel will form, and the ionization degree is higher than before.

The continuous application of impulse voltage results in a large amount of energy accumulation and temperature rise at the head of the rod electrode and the further increase of the ion density in the streamer channel, which eventually leads to the downward expansion of the intense ionization region in the form of the leader (Figure 19(c)). There may be leader branches in the leader development process, which have different ionization degrees and development paths. However, there must be at least one branch that develops downwards. When the leader length reaches about 1/2 of the gap length, the space electric field between the head of the leader and the plate electrode, and the ionization degree increase sharply, due to the shorter distance between the leader head and the plate electrode and the influence of the leader channel. With the final jump stage occurs, the leader discharge channel finally runs through the whole gap (Figure 19(d)).

C. THE NEGATIVE DISCHARGE

According to the nanosecond spatial-temporal distribution of the discharge process under the negative lightning impulse in 1m rod-plate air gap, the complete discharge process is proposed, as shown in Figure 20.

Under the negative standard lightning impulse, the initial electron collapse occurs near the rod electrode. When the voltage reaches high enough, firstly, an intense corona discharge area also will form above the head of the rod electrode (Figure 20(a)). Then the streamer will begin to develop downwards from the head of the rod electrode with the increase of the applied voltage (Figure 20(b)). The ionized free electrons move from the rod electrode to the plate electrode. Because of the uniform distribution of the electric field near the plate electrode, these electrons will not concentrate in certain region when they move towards the plate, and the streamer head diverges outwards and the whole ionization region is fan-shaped. Intense ionization regions appear mostly right below the head of the electrode and the outer edge of the streamer head, and the ion density in the middle part of the streamer channel is smaller.

After the penetrative streamer channel forms, the continuous intense ionization leads to the leader develops downwards (Figure 20(c)). The intense ionization region near the plate electrode may also form an upward leader, but the ionization degree of the upward leader is smaller and the development velocity is slower than those of the downward leader. When the leader length reaches about 1/2 of the gap length, the final jump occurs. And the gap is broken down (Figure 20(d)).

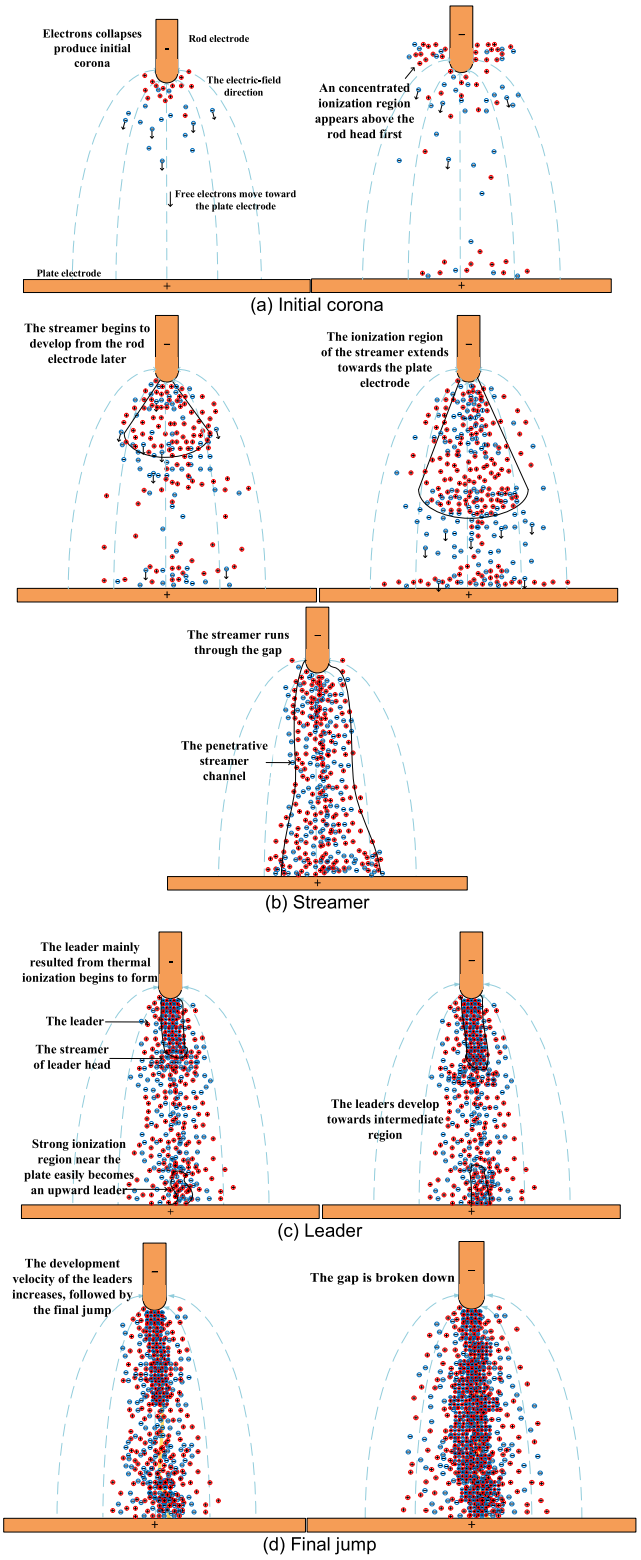

FIGURE 20. The breakdown discharge process of 1m rod-plate gap under the negative lightning impulse.

V. CONCLUSION

Based on the EMICCD, an experimental study on the nanosecond spatial-temporal distribution of the discharge process in 1 m rod-plate air gap under the standard

lightning impulse was carried out. The following are the conclusions.

(1) An improved method of the air gap discharge observation, using EMICCD camera, was proposed. The transient discharge process can be observed more clearly through changing the EMICCD time delay and the light intensity gain. The complete discharge development processes under different lightning impulses were reproduced well by image stitching.

(2) The breakdown discharge process in 1 m rod-plate air gap has four main stages, including initial corona, streamer, leader and final jump. Under the positive lightning impulse, the initial corona with weak discharge appears first. Then the streamer with a spherical ionization region will begin to develop. After a penetrative streamer channel formed, the visible leader develops from the rod electrode to the plate electrode. With the final jump stage occurs, the leader discharge channel finally runs through the whole gap.

(3) Under the negative lightning impulse, an intense corona discharge area will also form above the head of the rod electrode. The whole ionization region of the streamer is fan-shaped, which is quite different from that spherical ionization region under the positive impulse. These streamer differences during the discharge process in 1 m rod-plate air gap under the positive and negative lightning impulses have not been previously presented and analyzed systematically. After the streamer penetrates the discharge gap, the leader begins to develop downward from the rod electrode, and it is easy to produce the upward leader near the plate electrode under negative lighting impulse.

(4) The streamer forms and develops into a penetrative channel through the whole gap if the impulse voltage is high enough. However, if the streamer still cannot penetrate the entire gap when the applied impulse voltage exceeds the peak, the streamer will eventually dissipate and the gap cannot be broken down finally.

(5) Under the conditions of shorter air gap and stronger electric field relatively, the leader forms and development quickly after the first streamer run through the gap and there will not be an obvious reverse ion wave (second streamer). At the same time, no significant pulse current occurs during streamer discharge process.

ACKNOWLEDGMENT

The authors gratefully acknowledge all the members involved in the project, and the support of the National Engineering Laboratory in Kunming, China.

REFERENCES

[1] J. S. Townsend, *The Theory of Ionization of Gases by Collision*. London, U.K.: Constable & Company LTD, 1910.
[2] R. D. Townsend and D. L. Egar, "Rapid temperature reduction of thermal discharge," *J. Hydraul. Division*, vol. 101, no. 10, pp. 529–541, 1975.
[3] L. B. Loeb and J. M. Meek, "The mechanism of spark discharge in air at atmospheric pressure. II," *J. Appl. Phys.*, vol. 11, pp. 459–474, Sep. 1940.
[4] L. B. Loeb, "The mechanism of spark discharge in air at atmospheric pressure," *Science*, vol. 69, no. 1794, p. 509, 1929.
[5] W. F. Nash, "Electron avalanche and breakdown in gases, by H. Raether," *Contemp. Phys.*, vol. 6, p. 160, Dec. 1964.
[6] L. Zhang, Q. Zhang, S. Liu, F. Liu, L. Li, Y. Yin, W. Shi, and W. Chen, "Insulation characteristics of 1100 kV GIS under very fast transient overvoltage and lightning impulse," *IEEE Trans. Dielectr. Electr. Insul.*, vol. 19, no. 2, pp. 1029–1036, Jun. 2012.
[7] L. Zhang, Q. Zhang, Y. Yin, W. Shi, and W. Chen, "Voltage-time characteristics of long SF6 gap under VFTO and lightning impulse," *Gaodianya-Jishu/High Voltage Eng.*, vol. 39, no. 6, pp. 1396–1401, 2013.
[8] P. Lalande, A. Bondiou-Clergerie, P. Laroche, A. Eybert-Berard, J.-P. Berlandis, B. Bador, A. Bonamy, M. A. Uman, and V. A. Rakov, "Leader properties determined with triggered lightning techniques," *J. Geophys. Res. Atmos.*, vol. 103, no. D12, pp. 14109–14115, 1998.
[9] *Research on Long Air Gap Discharges at Les Renardières*, Les Renardières Group, Paris, France, 1972, vol. 23, pp. 53–157.
[10] *Research on Long Air Gap Discharges at Les Renardières-1973 results*, Les Renardières Group, Paris, France, 1974, vol. 35, pp. 47–156.
[11] *Positive Discharges in Long Air Gaps at Les Renardières-1975 Results and Conclusions*, Les Renardières Group, Paris, France, 1977, vol. 53, pp. 31–151.
[12] I. Gallimberti, "The mechanism of the long spark formation," *Le J. De Phys. Colloques*, vol. 40, no. C7, pp. 193–250, 1979.
[13] I. Gallimberti, G. Bacchiega, A. Bondiou-Clergerie, and P. Lalande, "Fundamental processes in long air gap discharges," *Comp. RendusPhys.*, vol. 3, pp. 1335–1359, Dec. 2002.
[14] T. Suzuki and K. Miyake, "Breakdown process of long air gaps with positive switching impulses," *IEEE Trans. Power App. Syst.*, vol. 94, no. 3, pp. 1021–1033, May 1975.
[15] R. T. Waters, R. E. Jones, and T. E. Allibone, "The impulse breakdown voltage and time-lag characteristics of long gaps in air II. The negative discharge," *Philos. Trans. Roy. Soc. London A, Math. Phys. Sci.*, vol. 256, no. 1069, pp. 213–234, 1964.
[16] V. B. Lebedev, G. G. Feldman, and B. N. Gorin, "Test of the image converter cameras complex for research of discharges in long air gaps and lightning," Bifo Company, Moscow, Russia, Tech. Rep.
[17] R. Ackermann, G. Méchain, G. Méjean, R. Bourayou, M. Rodriguez, K. Stelmaszczyk, J. Kasparian, J. Yu, E. Salmon, S. Tzortzakis, Y.-B. André, J.-F. Bourrillon, L. Tamin, J.-P. Cascelli, C. Campo, C. Davoise, A. Mysyrowicz, R. Sauerbrey, L. Wöste, and J.-P. Wolf, "Influence of negative leader propagation on the triggering and guiding of high voltage discharges by laser filaments," *Appl. Phys. B, Lasers Opt.*, vol. 82, no. 4, pp. 561–566, 2006.
[18] T. Reess, P. Ortega, A. Gibert, P. Domens, and P. Pignolet, "An experimental study of negative discharge in a 1.3 m point-plane air gap: The function of the space stem in the propagation mechanism," *J. Phys. D, Appl. Phys.*, vol. 28, no. 11, p. 2306, 2017.
[19] P. Domens, A. Gibert, J. Dupuy, and B. Hutzler, "Propagation of the positive streamer-leader system in a 16.7 m rod-plane gap," *J. Phys. D, Appl. Phys.*, vol. 24, no. 10, p. 1748, 2000.
[20] S. Gu, W. Chen, J, Chen, H. He, and G. Qian, "Observation of the streamer-leader propagation processes of long air-gap positive discharges," *IEEE Trans. Plasma Sci.*, vol. 38, no. 2, pp. 214–217, Feb. 2010.
[21] W. Chen, S. Gu, S. Xie, B. Sun, H. He, J. Chen, J. He, G. Qian, and N. Xiang, "Experimental observation technology for long air gap discharge," *Proc. Chin. Soc. Elect. Eng.*, vol. 32, no. 10, pp. 13–21, 2012.
[22] S. Xie, J. Li, T. Luo, Y. Zhang, J. He, C. Wu, and Y. Yue, "Formation and characteristics of negative stepped leaders in 4–10 m long air gap discharges," in *Proc. Int. Conf. Lightning Protection*, Sep. 2016, pp. 1–4.
[23] S. J. Xie, S.-Q. Gu, W.-J. Chen, J.-H. Chen, G.-J. Qian, and H. He, "Characteristics of the stepped leader of negative discharge in long air gaps," *High Voltage Eng.*, vol. 35, no. 12, pp. 2953–2957, 2009.
[24] S. Xie, H. He, N. Xiang, S. Gu, J. Wan, W. Chen, H. Jinliang, J. Chen, G. Qian, and Z. Cheng, "Experimental study on the discharge processes of rod-rod air gap under switching impulse voltage," *High Voltage Eng.*, vol. 38, no. 8, pp. 2083–2090, 2012.
[25] Y. An, Y. Hu, R. Xian, B. He, X. Wen, L. Lan, Y. Wang, and E. Shenglong, "Breakdown characteristics of different air gaps with negative switching impulse," in *Proc. IEEE Int. Conf. High Voltage Eng. Appl.*, Sep. 2016, pp. 1–4.
[26] Y. Wang, Y. An, E. Shenglong, X. Wen, L. Lan, W. Chen, M. Dai, Z. Li, and Q. Ye, "Statistical characteristics of breakdowns in long air gaps at negative switching impulses," *IEEE Trans. Dielectr. Electr. Insul.*, vol. 23, no. 2, pp. 779–786, Apr. 2016.

[27] R. Zeng, Z. Li, Z. Yu, C. Zhuang, and J. He, "Study on the influence of the DC voltage on the upward leader emerging from a transmission line," *IEEE Trans. Power Del.*, vol. 28, no. 3, pp. 1674–1681, Jul. 2013.

[28] Y. Cui, R. Zeng, C. Zhuang, X. Zhou, Z. Wang, and S. Chen, "The dynamic expansion of positive leaders observed using Mach–Zehnder interferometry in a 1-m air gap," 2018, *arXiv:1801.04664*. [Online]. Available: https://arxiv.org/abs/1801.04664

[29] X. Zhou, R. Zeng, Z. Li, and C. Zhuang, "A one-dimensional thermo-hydrodynamic model for upward leader inception considering gas dynamics and heat conduction," *Electr. Power Syst. Res.*, vol. 139, pp. 16–21, Oct. 2016.

[30] X. Zhou, R. Zeng, Z. Li, and C. Zhuang, "Upward leader inception criterion considering gas kinetic process and heat conduction," in *Proc. Int. Conf. Lightning Protection (ICLP)*, Oct. 2014, pp. 1960–1963.

[31] P. T. Medeiros and S. R. Naidu, "Positive and negative lightning impulse breakdown of rod-plane gaps in nitrogen," in *Proc. Conf. Elect. Insul. Dielectric Phenomena-Annu. Rep.*, Oct. 2016, pp. 48–53.

[32] S. Chen, "The observation and 3D modelling of long positive streamers in air," in *Proc. Int. Symp. High Voltage Eng.*, 2013, pp. 1–6.

[33] S. Chen, R. Zeng, and C. Zhuang, "The diameters of long positive streamers in atmospheric air under lightning impulse voltage," *J. Phys. D, Appl. Phys.*, vol. 46, no. 37, 2013, Art. no. 375203.

[34] A. Shirvani, W. Schufft, H.-P. Pampel, and U. Schmidt, "Spatial-temporal investigation of breakdown of long air gaps by lightning voltages up to 2.4 MV," in *Proc. IEEE Elect. Insul. Conf.*, Jun. 2013, pp. 351–355.

[35] A. Shirvani, "Ein beitrag zum entladungsverhalten langer luftfunkenstrecken bei blitzspannung," Ph.D. dissertation, Chemnitz Univ. Technol., Chemnitz, Germany, 2014.

[36] P. O. Kochkin, C. V. Nguyen, A. P. J. van Deursen, and U. Ebert, "Experimental study of hard X-rays emitted from metre-scale positive discharges in air," *J. Phys. D, Appl. Phys.*, vol. 45, no. 42, 2012, Art. no. 425202.

[37] P. Kochkin, N. Lehtinen, A. P. J. van Deursen, and N. Østgaard, "Pilot system development in metre-scale laboratory discharge," *J. Phys. D, Appl. Phys.*, vol. 49, no. 42, 2016, Art. no. 425203.

[38] Y. Liao, C. Gao, G. Wang, R. Li, G. Lu, and R. Zeng, "The technology characteristics and research items of high altitude UHV outdoor test field at Kunming," (in Chinese), *Southern Power Syst. Technol.*, vol. 5, no. 6, pp. 29–32, 2011.

[39] Y.-S. Yue and J.-J. He, "Digital time-resolved optical measurement of discharge currents in long air gaps," *Rev. Sci. Instrum.*, vol. 84, no. 8, 2013, Art. no. 085107.

[40] X. Zhao, G. Liu, L. Jia, H. Cai, B. Luo, Y. Zhang, H. Chen, and J. He, "Breakdown characteristics of a 220-kV composite insulator string under short tail lightning impulses based on the discharge current and images," *IEEE Trans. Power Del.*, vol. 33, no. 6, pp. 3211–3217, Dec. 2018.

[41] X. Zhao, L. Liu, X. Wang, L. Liu, L. Qu, L. Jia, J. He, B. Luo, and H. Chen "On the velocity-current relation of positive leader discharges," *Geophys. Res. Lett.*, vol. 46, pp. 512–518, Jan. 2019.

[42] *High-Voltage Test Techniques Part 1: General Definitions and Test Requirements*, Standard IEC 60060-1, 1989.

[43] *High-Voltage Test Techniques—Part 2: Measuring Systems*, Standard IEC 60060-2, 2010.

[44] *High-Voltage Test Techniques-Part II: Measuring System*, China Standard GB/T 16927.2-2013, IS 2071-1, Chinese National Standard, Beijing, China, 2013.

[45] Y. Zhang, "Lightning flashover performance test and flashover criterion study of insulators in a 110 kV true type tower at high altitude areas," *Power System Technol.*, vol. 43, no. 1, pp. 340–348, 2019.

[46] J. Yang *et al.*, "Research on the flashover performance of the composite insulators in cup-tower under the impact of short-wave in high altitude area," *High Voltage Eng.*, vol. 45, no. 3, pp. 768–773, 2019.

[47] Y. Han, Y. Zhang, Y. Ruan, J. Yang, W. Zheng, G. Liu, H. Cai, and L. Li, "Study on influencing factors of insulators flashover characteristics on the 110 kV true tower under the lightning impulse," *IEEE Access*, vol. 6, pp. 66536–66544, 2018.

[48] P. O. Kochkin, A. P. J. van Deursen, and U. Ebert, "Experimental study of the spatio-temporal development of metre-scale negative discharge in air," *J. Phys. D, Appl. Phys.*, vol. 47, no. 14, p. 145203, Mar. 2014.

[49] R. Morrow and N. Sato, "The discharge current induced by the motion of charged particles in time-dependent electric fields; Sato's equation extended," *J. Phys. D, Appl. Phys.*, vol. 32, no. 5, p. L20, 1999.

[50] Y.-N. Geng, R. Zeng, J.-L. He, and B. Wang, "Pre-breakdown current measurements from high voltage electrode of rod-plane gap under lightning impulse voltage," *High Voltage Eng.*, vol. 37, no. 4, pp. 854–859, 2011.

YAQI ZHANG received the B.Sc. degree from the Changsha University of Science and Technology, China, in 2015. She is currently pursuing the Ph.D. degree with the South China University of Technology. Her research interests include gas discharge and insulation coordination.

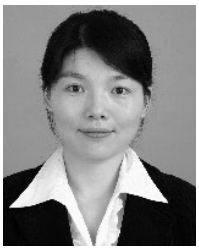

YONGXIA HAN received the B.Sc., M.Sc., and Ph.D. degrees in electrical and electronic engineering from the Huazhong University of Science and Technology (HUST), Wuhan, China, in 2004, 2006, and 2009, respectively. She is currently an Associate Professor and the Doctoral Supervisor with the South China University of Technology. Her research interests include gas discharge, electromagnetic transient analysis in LCC/VSC HVDC/MVDC, and overvoltage and insulation coordination in power systems. She is a member of the IEEE.

WENBO ZHENG is currently pursuing the degree with the South China University of Technology. His main research interest includes long air gap discharge.

JIE YANG is currently pursuing the degree with the South China University of Technology. His research interests include gas discharge and insulation coordination.

Lu Qu received the B.Sc. and M.Sc. degrees in electrical engineering from Jilin University, Changchun, China, in 2010 and 2013, respectively, and the Ph.D. degree in electrical engineering in high voltage technology from Wuhan University, Wuhan, China, in 2017. He is currently a Senior Engineer with the Electric Power Research Institute, China Southern Power Grid. His research interests include power system lightning protection and lightning protection of wind turbine.

GANG LIU received the Ph.D. degree in high voltage and insulation technology from the Huazhong University of Science and Technology, Wuhan, China, in 2011. He is currently a Senior Engineer with the Electric Power Research Institute, China Southern Power Grid. He has been working on overvoltage calculations and high voltage experiments.

XIANGEN ZHAO received the B.Sc. and Ph.D. degrees from the Huazhong University of Science and Technology, Wuhan, China, in 2011 and 2017, respectively. He currently holds a Postdoctoral position with the Electric Power Research Institute, China Southern Power Grid. His main research interests include the observation and simulation of the long air-gap discharge in laboratory and the lightning to tall buildings in nature. He is currently working on the projects related to the positive leader branching, re-illumination of positive leader, and relaxation phase of the discharge channel.

LICHENG LI received the B.S. degree from the Department of Electrical Engineering, Tsinghua University, Beijing, China, in 1967. He has been working with the HVDC area for many years. He is currently an Academician with the Chinese Academy of Engineering (CAE), and a Professor and a Doctoral Supervisor with the South China University of Technology. He is also the Secretary of the Expert Committee of China Southern Power Grid.